of sparse signals and faithfully reconstruct the original signals back from fewer compressive measurements. It has been applied in many fields, including speech enhancement [14], magnetic resonance imaging [15], wireless sensor network [16], etc. Moreover, several CS-based methods have been proposed for GNSS signal acquisition. He et al. [17] used the sparse matrix to compress the spread spectrum signal and reconstructed the compressed signal based on the greedy algorithm. Kong et al. [18] proposed two-stage compression of GNSS signal by the Walsh–Hadamard matrix, which achieved fast acquisition with fewer correlators than traditional acquisition methods. Chang et al. [19] combined CS with subspace to enhance the acquisition performance of GNSS signal when there are a lot of interferences. He et al. [20] designed a sparse dictionary based on the features of the GLONASS navigation signal and modified the greedy reconstruction algorithm to achieve fast acquisition. However, the above algorithms are based on the conventional frequency search method with a fixed bandwidth, which results in low acquisition probabilities under high dynamic conditions.

In this paper, a GNSS signal acquisition algorithm based on two-stage compression of the code-frequency domain is proposed, which divides the Doppler frequency offset into multiple intervals, and the multiple frequency points are compressed and searched in every interval at the same time to increase the correlation bandwidth. This method can overcome the limitations of the conventional Doppler frequency search and is suitable for fast acquisition in high dynamics.

The rest of this paper is organized as follows. Section 2 introduces the compression acquisition theory and the problems of the compression acquisition algorithm in a highly dynamic environment. Section 3 proposes the model of two-stage compression and theoretically analyzes the advantages of the proposed method, including computational complexity and detection probability. Section 4 compares the performance of the proposed algorithm with other acquisition algorithms and discusses the performance with different key parameters. Section 5 concludes this paper.

2. Code-Domain Compression Acquisition Algorithm

2.1. Sparsification of GNSS Signal

The incoming digital down-converted GNSS intermediate frequency (IF) signal can be expressed as [21]

$$r(n) = Ad(n)c(n-\tau)\exp[j(2\pi(f_{\mathrm{IF}} + f_{\mathrm{d}})nT_{\mathrm{s}} + \varphi)] + v(n) \tag{1}$$

where A is the signal amplitude, d is the signal data, c is the spreading code, f_{IF} is the intermediate frequency, f_{d} is the Doppler frequency offset, T_{s} is the sampling interval, τ is the code phase, v is the noise, and φ is the unknown carrier phase.

From the previous work, we know GNSS signal acquisition is possible at a low sampling rate by employing CS theory to compress the raw GNSS signal data using a measurement matrix [22], which can be expressed as

$$\mathbf{y} = \mathbf{\Phi} \cdot \mathbf{x} \tag{2}$$

where $\mathbf{x}$ is the original signal, $\mathbf{y}$ is the measurement vector, $\mathbf{\Phi} \in R^{M\times N}$ is the measurement matrix, N is the signal length, M is the measurement length, and $M << N$.

The premise of CS is that the signal is sparse. However, most of the real signals are not sparse but can be expressed as

$$\mathbf{x} = \mathbf{\Psi} \cdot \mathbf{a} \tag{3}$$

where $\mathbf{\Psi}$ is called the sparse basis of the signal, $\mathbf{a}$ is a sparse vector.

Shifting the spreading code vector $\mathbf{c} = [c(0), c(1), \cdots, c(NK-1)] \in R^{NK\times 1}$ to get the code matrix $\mathbf{C}$

$$\mathbf{C} = [\mathbf{c}_0, \mathbf{c}_1, \cdots, \mathbf{c}_{N-1}] = \begin{bmatrix} c(0) & c(1) & \cdots & c(2K-1) \\ c(K) & c(K+1) & \cdots & c(3K-1) \\ \vdots & \vdots & \ddots & \vdots \\ c[(N-1)K] & c[(N-1)K+1] & \cdots & c[(N+1)K-1] \end{bmatrix} \tag{4}$$

where N is the amount of points in the FFT, and $N = 2K$.

Padding zeros to the end of the incoming signal $r(n)$ to increase its length to $2K$, which can solve the problem of non-periodicity after block processing of spreading code and reduce computation effectively [23]. It can be described as

$$\mathbf{r} = [r(0), r(1), \cdots, r(K-1), 0_{1\times K}]^{\mathrm{T}} \tag{5}$$

Then, correlating the padded signal vector $\mathbf{r}$ with the local spreading code matrix $\mathbf{C}$, we can obtain the correlation vector $\mathbf{X}$

$$\mathbf{X} = \mathbf{C} \cdot \mathbf{r} \tag{6}$$

The acorrelation function (CF) of the incoming signal and the spreading code can be described as

$$X_i = < \mathbf{c}_n, \mathbf{r} > = \sum_{i=0}^{2K-1} c(i+n) r(i) = \begin{cases} v + 2AK\left(1 - \frac{|\tau|}{T_c}\right), & |\tau| \le T_c \\ v, & |\tau| > T_c \end{cases} \tag{7}$$

where X_i is the ith element of the correlation vector $\mathbf{X}$, $\mathbf{c}_n$ is the nth row of the code matrix $\mathbf{C}$, $< \cdot >$ is the discrete-time convolution operation, T_c is the chip time, $2AK$ is the maximum peak value.

As shown in Figure 1, the correlation result $\mathbf{X}$ can be considered sparse if $|2AK| >> |v|$ in Equation (7).

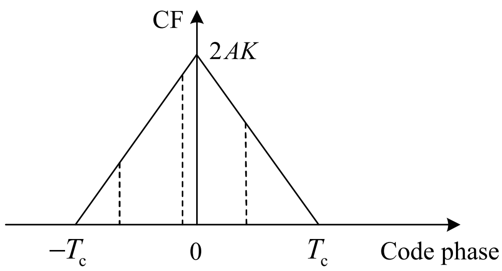

Figure 1. Model of correlation output.

2.2. Code-Domain Compression Acquisition

According to Equations (2) and (6), we can use the measurement matrix $\mathbf{\Phi}$ to compresses the $N \times 1$ dimensional correlation result $\mathbf{X}$ to obtain the $M \times 1$ dimensional measurement data $\mathbf{Y}$

$$\underset{M\times 1}{\mathbf{Y}} = \underset{M\times N}{\mathbf{\Phi}} \cdot \underset{N\times 1}{\mathbf{X}} = \underset{M\times N}{\mathbf{\Phi}} \cdot \underset{N\times 2K}{\mathbf{C}} \cdot \underset{2K\times 1}{\mathbf{r}} \tag{8}$$

The measurement matrix $\mathbf{\Phi}$ will be helpful for signal reconstruction when restricted isometry property (RIP) criteria is satisfied. In other words, each column is a unit vector, and the sum of squares of all columns meets the Welch bound [24,25]

$$\sum_{i=1}^{N} \sum_{j=1}^{N} \left|\langle \phi_i, \phi_j \rangle\right|^2 \ge \frac{N^2}{M} \tag{9}$$

The FFT-based parallel search engine is adopted to acquire the correlation peak, which converts time-domain convolution operation into frequency-domain multiplication.

The FFT of $\mathbf{\Phi} \cdot \mathbf{C}$ are taken and multiplied by the FFT of the $\mathbf{r}$, and then taken the inverse FFT (IFFT) to obtain $\mathbf{Y}$.

The correlation result $\mathbf{X}$ can be reconstructed from $\mathbf{Y}$ through some reconstruction algorithms, which can be described as follows

$$\min \| \mathbf{X}\|_0 \quad \text{s.t.} \quad \mathbf{Y} = \mathbf{\Phi} \cdot \mathbf{X} \tag{10}$$

where $\| \cdot\|_0$ means the l_0 norm which counts the number of nonzero elements.

The l_0 norm is a NP-hard problem, which can be converted into l_2 norm if the measurement matrix $\mathbf{\Phi}$ meets the RIP condition.

$$\min \| \mathbf{X} \|_2^2 \quad \text{s.t.} \quad \mathbf{Y} = \mathbf{\Phi} \cdot \mathbf{X} \tag{11}$$

where $\| \cdot\|_2$ is the l_2 norm, also known as the Euclidean norm, which is used as a standard quantity for measuring a vector difference [26].

The least square method (LSM) is used to reconstruct the elements from the measurement data $\mathbf{Y}$ [27].

$$\mathbf{X} = \mathbf{\Phi}^{\mathrm{T}}(\mathbf{\Phi}\mathbf{\Phi}^{\mathrm{T}})^{-1}\mathbf{Y} \tag{12}$$

The correct code phase and Doppler frequency offset are determined by comparing the first K elements from the correlation result $\mathbf{X}$. Replacing the circular correlation with a compressed reconstruction in this method decreases the number of correlators from $N+1$ to $M+1$ [28].

As we know, the correlation function $R(\tau, f_{\mathrm{d}})$ of the spreading code can be described as follows [29]

$$R(\tau, f_{\mathrm{d}}) = 2AK\left(1 - \frac{|\tau|}{T_{\mathrm{c}}}\right)\frac{\sin[\pi(f_{\mathrm{d}} - f_i)2KT_{\mathrm{s}}]}{\sin[\pi(f_{\mathrm{d}} - f_i)T_{\mathrm{s}}]}\exp[j\gamma(\varphi)] \tag{13}$$

where $\gamma(\varphi) = \pi(f_{\mathrm{d}} - f_i)(2K-1)T_{\mathrm{s}} + \varphi$, f_i is the Doppler frequency hypothesis.

We can find that $R(\tau, f_{\mathrm{d}})$ is affected by the Doppler frequency as a $\mathrm{sinc}(\cdot)$ function [29], and the zero of its main lobe is located at

$$f_{\mathrm{d}} = \frac{\pm 1}{KT_{\mathrm{s}}} + f_i \tag{14}$$

The correlation bandwidth B_{c} denotes

$$B_{\mathrm{c}} = \frac{2}{KT_{\mathrm{s}}} \tag{15}$$

Hence the Doppler frequency offset range in each search is obtained as

$$f_{\mathrm{d}} \in \left[\frac{-1}{KT_{\mathrm{s}}} + f_i, \frac{1}{KT_{\mathrm{s}}} + f_i\right] \tag{16}$$

where the search accuracy is $1/(KT_{\mathrm{s}})$.

In above algorithm, the acquisition is serial in the frequency domain, and it will take a long time to acquire the Doppler frequency in high dynamics.

3. Code-Frequency Two-Stage Compression Acquisition

In this section, we introduce a new frequency domain compression to preprocess the incoming signal to reduce the influence of large Doppler frequency offset.

3.1. Frequency Domain Compression Preprocessing

The incoming signal is multiplied with $\exp[j2\pi(f_{\mathrm{o}}^i + f_{\mathrm{c}}^l)]$ to produce the mapped signal $r_l'(n)$

$$r_l'(n) = r(n)\exp[j2\pi(f_{\mathrm{o}}^i + f_{\mathrm{c}}^l)nT_{\mathrm{s}}] \tag{17}$$

where f_c^l is the multiple carrier frequency bins, $l \in \{0, 1, 2, \ldots, L-1\}$, L is the frequency compression ratio (FCR), the frequency search step $f_{\text{step}} = f_c^{l+1} - f_c^l$, f_o^i is the starting frequency in once frequency compression search, $i \in \{0, 1, 2, \ldots, I-1\}$, I is the number of sub-carrier bins, the frequency compression steps $f_o^{i+1} - f_o^i = L \cdot f_{\text{step}}$.

Hence the Doppler frequency offset can be expressed as

$$f_d = I \cdot L \cdot f_{\text{step}} \tag{18}$$

Figure 2 shows the process of the mapping and overlapping-based carrier frequency searching technique. We divide the Doppler frequency offset f_d into I sub-carrier frequency bins and search for L sub-frequency points separated by f_{step} simultaneously.

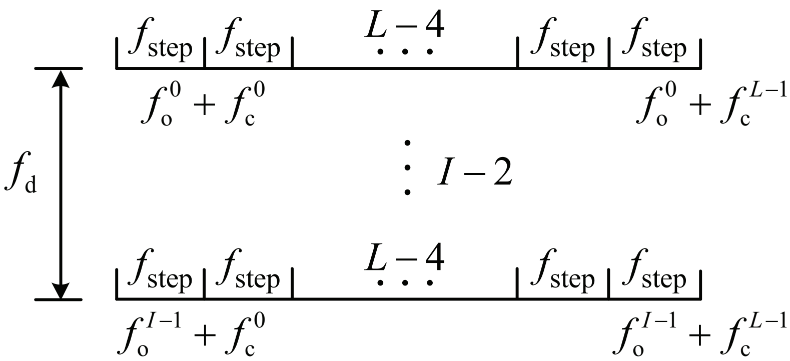

Figure 2. Schematic diagram of frequency domain compression processing.

From Equation (13), we can see that if the Doppler frequency is greater than the correlation bandwidth $B_c = 2/(KT_s)$, the correlation value is attenuated seriously. Accordingly, the frequency search step should satisfy $f_{\text{step}} \leq B_c/2$, making sure at least two neighboring acquisition frequency points are located within the correlation bandwidth B_c, which is beneficial to enhancing the acquisition performance, as shown in Figure 3a. However, if $f_{\text{step}} > B_c$, the neighbor acquisition frequency exceeds the correlation bandwidth B_c, causing the correlation value decrease and the acquisition failure, as illustrated in Figure 3b.

Then, the mapped signals which correspond to the same code phase are overlapped together. Consequently, we obtain the preprocessed incoming signal

$$r_l''(n) = \sum_{l=0}^{L-1} r_l'(n) \tag{19}$$

The correlation bandwidth of the comprssion acquisition is improved by frequency domain preprocessing, which can be expressed as

$$B_c' = (L-1) f_{\text{step}} + B_c \tag{20}$$

Compared with the traditional Doppler frequency search method, the L frequency bins are searched simultaneously in this method, which can reduce search number and acquisition time.

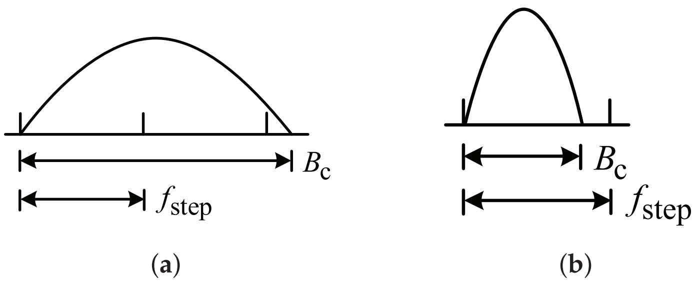

Figure 3. The relationship between frequency search step and correlation bandwidth: (**a**) $f_{\text{step}} \leq B_c/2$; (**b**) $f_{\text{step}} > B_c$.

3.2. Algorithm Process

The detailed and straightforward processes of proposed GNSS acquisition algorithm are shown in Algorithm 1 and Figure 4.

Algorithm 1 The proposed GNSS acquisition algorithm.

Input: Incoming signal, $r(n)$; Spreading code vector, $\mathbf{c}_0$; Measurement matrix, $\mathbf{\Phi}$; Decision threshold, V_t;

Output: Code phase, τ; Doppler frequency offset, f_d;

1: Mapping incoming signal $r(n)$ to different carrier frequencies f_o^i;
2: Overlapping the mapped signals to the same code phase to obtain $r_l''(n)$;
3: Padding zeros to the end of the mapped signals $r_l''(n)$ to form a signal vector $\mathbf{r}''$;
4: Shifting spreading code vector $\mathbf{c}_0$ to obtain the code matrix $\mathbf{C}$;
5: Performing FFT operation to find out the measurement data $\mathbf{Y}$;
6: Using the greedy algorithm to obtain the correlation result $\mathbf{X}$;
7: Comparing the first K elements from the correlation result $\mathbf{X}$ with the threshold V_t to obtain the code phase τ and Doppler shift f_d;
8: **return** τ, f_d;

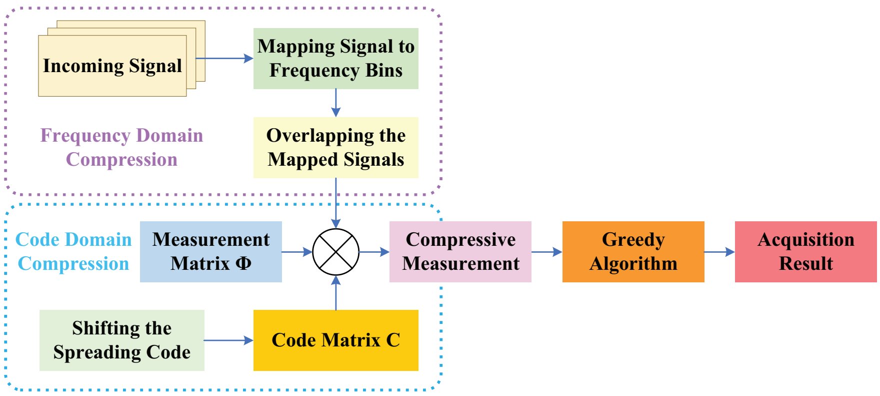

Figure 4. GNSS signal acquisition based on code-frequency compression.

3.3. Detection Probability Analysis

Assuming a partial Hadamard matrix is adopted as measurement matrix to assess the performance of the proposed algorithm, the following two hypotheses determine the test statistic for signal detection

$$\tilde{\mathbf{y}} = \begin{cases} \mathbf{\Phi}_1 \mathbf{w} & H_0 \\ \mathbf{\Phi}_1(\mathbf{x} + \mathbf{w}) & H_1 \end{cases} \tag{21}$$

where $\mathbf{\Phi}_1 \in \mathbf{R}^{(MT_p/\alpha_c) \times N}$ denotes a random partial Hadamard matrix, α_c is the maximum subsampling factor, T_p is the spreading spectrum period, H_1 denotes the signal is present and correctly aligned with the local replica, H_0 denotes the signal is absent or not correctly aligned with local replica.

Consequently, the probability density function of $\tilde{\mathbf{y}}$ under hypothesis H_1 is shown as follows:

$$p\left(\tilde{\mathbf{y}} \mid \widehat{\widehat{\mathbf{x}}}, H_1\right) = \frac{1}{(2\pi)^{(M/\alpha_c)/2}\left|\sigma^2\boldsymbol{\Phi}_1\boldsymbol{\Phi}_1^{\mathrm{T}}\right|^{1/2}} \exp\left[-\frac{1}{2}(\mathbf{W})^{\mathrm{T}}\left(\sigma^2\boldsymbol{\Phi}_1\boldsymbol{\Phi}_1^{\mathrm{T}}\right)^{-1}(\mathbf{W})\right] \tag{22}$$

where $\mathbf{W} = \tilde{\mathbf{y}} - \mathbf{D}\widehat{\mathbf{x}}$, $\mathbf{D}{=}\boldsymbol{\Phi}_1 \cdot \Psi$, and $\widehat{\mathbf{x}}$ denotes

$$\widehat{\mathbf{x}} = (\boldsymbol{\Phi}_1\boldsymbol{\Phi}_1^{\mathrm{T}})^{-1}\boldsymbol{\Phi}_1^{\mathrm{T}}\tilde{\mathbf{y}} \tag{23}$$

The $\widehat{\widehat{\mathbf{x}}}$ denotes the maximum likelihood estimation (MLE) of $\mathbf{x}$ under H_1, which is shown as

$$\widehat{\widehat{\mathbf{x}}} = \left(\mathbf{D}^{\mathrm{T}}(\sigma^2\boldsymbol{\Phi}_1\boldsymbol{\Phi}_1^{\mathrm{T}})^{-1}\mathbf{D}\right)^{-1}\mathbf{D}^{\mathrm{T}}(\sigma^2\boldsymbol{\Phi}_1\boldsymbol{\Phi}_1^{\mathrm{T}})^{-1}\tilde{\mathbf{y}} \tag{24}$$

If the threshold η is selected to attain the required false alarm probability, the detection performance can be obtained as

$$P_d = \Pr(\Gamma_{\tilde{\mathbf{y}}} > \eta \mid H_1) = Q_{\tilde{\chi}^{2\lambda}_{MT_{\mathrm{p}}/\alpha_c}(\lambda)}(\eta) \tag{25}$$

where $\Gamma_{\tilde{\mathbf{y}}}$ is a noncentral chi-squared distribution with MT_{p}/α_c degrees of freedom, which is expressed as

$$\Gamma_{\tilde{\mathbf{y}}} = \tilde{\mathbf{y}}^{\mathrm{T}}(\sigma^2\boldsymbol{\Phi}_1\boldsymbol{\Phi}_1^{\mathrm{T}})^{-1}\mathbf{D}\left(\mathbf{D}^{\mathrm{T}}(\sigma^2\boldsymbol{\Phi}_1\boldsymbol{\Phi}_1^{\mathrm{T}})^{-1}\mathbf{D}\right)^{-1}\mathbf{D}^{\mathrm{T}}(\sigma^2\boldsymbol{\Phi}_1\boldsymbol{\Phi}_1^{\mathrm{T}})^{-1}\tilde{\mathbf{y}} \tag{26}$$

where λ is a non-centrality parameter specified by

$$\lambda = \sigma^{-2}(\mathbf{x}^{\mathrm{T}})^{-1}\boldsymbol{\Phi}_1^{\mathrm{T}}\left(\boldsymbol{\Phi}_1\boldsymbol{\Phi}_1^{\mathrm{T}}\right)^{-1}\boldsymbol{\Phi}_1\mathbf{x} \tag{27}$$

3.4. Complexity Analysis

The complexity of the proposed algorithm consists of three parts: frequency domain compression preprocessing, code domain compression, and signal reconstruction, of which the first and third are the main parts, and the second part can be ignored as the elements of the measurement matrix are -1 or 1. In this paper, we chose the orthogonal matching pursuit (OMP) algorithm for signal reconstruction, whose complexity is $O(N \cdot (\log_2(N))^2)$ [30,31]. Table 1 gives the complexities of the serial acquisition algorithm, the PMF-FFT acquisition algorithm, the code-compression (CC) acquisition algorithm [26] and the proposed code-frequency compression (CFC) acquisition algorithm.

Table 1. Table of algorithm complexities.

Acquisition Algorithm	Complexity
Serial acquisition algorithm	$O(N^2 \cdot I \cdot L)$
PMF-FFT acquisition algorithm	$O(N \cdot (L \cdot \log_2(L) + N))$
CC acquisition algorithm	$O(N \cdot (\log_2(N))^2 \cdot I \cdot L)$
CFC acquisition algorithm	$O(N \cdot (\log_2(N))^2 \cdot I)$

4. Simulation Results

The GPS L1 signal is adopted to evaluate the performance of the proposed method. Set the data rate R_{b} = 50 bps, the code rate R_{c} = 1.023 Mcps, the sampling rate $f_{\mathrm{s}} = 2R_{\mathrm{c}}$, the code phase τ = 400, the code length N = 1024, the measured length M = 768, and the Doppler frequency offset range is ±80 KHz.